Journal of Applied Sciences Research, 7(7): 1222-1232, 2011
ISSN 1995-0748
This is a refereed journal and all articles are professionally screened and reviewed

ORIGINAL ARTICLES

Hydrodynamic Interaction Between Two Spheres in Newtonian and non Newtonian Fluid

[1]Abbas H. Sulaymon, [2]Sawsan A. M. Mohammed and [1]Abeer I. Alwared

[1]Environmental Engineering Department-College of Engineering-University of Baghdad - Iraq.
[2]Chemical Engineering Department-College of Engineering-University of Baghdad - Iraq.

ABSTRACT

Experiments have been performed on the hydrodynamic interaction between two spheres in Newtonian and non Newtonian fluid. Glycerin and polyacrylamide solution were used in which the interacting spheres were suspended. Comparison of the results shows that the ratio of drag coefficient in power-law fluid is exponentially dependent on the separation distance and is strongly related to the particle Reynolds number, but nearly independent of the power-law index within the range of the present investigation (0.61 - 0.834). The change of the history force with time for Newtonian and non Newtonian fluid shows it decays faster then t^{-2} and that due to the rheological properties of the non Newtonian fluid which requires the two spheres to be separated farther than in Newtonian fluid in order to approach the virtual mass coefficient of a single sphere.

Key words: Hydrodynamic interaction, Two spheres interaction, Newtonian and non Newtonian fluids.

Introduction

Accurate prediction of particle (or droplet) dispersion is important in many two phase flow system. The resisted motion of spherical objects (and small equivalently shaped particles) falling through incompressible Newtonian fluid is relevant to many situations of practical interest, such as the precipitation of raindrops and hydrometers, the gravitational settling of red blood cells.

An extensive and rapidly increased number of industrial applications of multiphase flow involve particle motions in non-Newtonian flow. Typical cases are exemplified by crude oil flow with rocks, sands or natural gas; bubbles entrainment and migration in plastic casting processes; polymeric flow with catalytic particles; bio fluid flow in three-phase fluidized beds; and aseptic processing of particulate food in liquid (Zhu, 2003).

All of the above applications call for an in-depth understanding of particle dynamics in non-Newtonian flow, especially the information of drag force of interacting particles.

The earliest theoretical work on the force experienced by a sphere suspended in a Newtonian fluid was dated back in 1901 when Stokes rigorously derived the famous Stokes law to calculate the drag force on a single rigid sphere in an unbounded creeping Newtonian flow. Drag force of multi-spheres in a viscous fluid flow have been extensively investigated.

Complete solution for the slow motion of two spheres parallel to their line of centers in an unbounded viscous fluid was dated back to 1926 (Stimson, 1926), while the theoretical treatment of Stokes motions of three or more spheres delivered in1959. Payne and Pell (1960) solved the Stokes equation for the slow motion of several axially symmetric bodies in an unbounded viscous fluid.

The drag force was numerically investigated on the simple and periodic arrays of spheres in a Stokes flow by formulating the problem as a set of two-dimensional integral equations (Zick, 1982). In order to account for the wall effect the drag force was numerically computed on two spherical particles translating in a cylindrical tube filled with an incompressible viscous fluid, from this calculation, interaction and wall correction factors based on the distance between particles, the distance between the particles and the tube wall were proposed (Greenstein, 1980).

Corresponding Author: Abbas H. Sulaymon, Environmental Engineering Department-College of Engineering-University of Baghdad - Iraq.

If particles are located randomly in a particulate fluid system, the most important hydrodynamic interactions are those between a pair of particles. However, in the case of a pair of particles sedimenting vertically one above the other in an unbounded fluid, the difference between the forces on the leading and trailing spheres can not be explained by an analysis based on the Stokes equation. Hence, an asymptotic analysis was proposed to treat the hydrodynamic interaction of two spheres moving in an unbounded fluid at small but finite Reynolds number in which the inertia effect was taken into account (Kaneda,1982). However, these treatments can only be applied to cases with large separation distance between particles in small Reynolds numbers. It is realized that the typical distance of strong interaction of a pair of particles is less than twice particle diameter. In addition, for most applications in particulate multiphase flow, the particle Reynolds number based on the isolated particle terminal velocity and particle diameter is typically in a range from tens to several hundreds. For example, at a particle Reynolds number from 10 to 200, the corresponding sizes of glass beads vary from 230 μm to 1.1 mm in water and from 130 to 650 μm in air. Hence, the Reynolds number range of practical significance to a multiphase flow system may be far beyond the Stokes regime. For such a case, inertia effect and wake effect must be taken into account (Zhu, 1994).

The terminal velocity for two spheres falling in viscous liquid were greater than that of an isolated sphere as concluded from experimental investigation which lead to the drag force of any one of the two spheres is reduced by the sphere interaction (Happel, 1960).

Realizing the importance of the direct measurements of drag force of interacting particles, used the pendulum method and water channel flow was used to measure the drag force at a particle Reynolds number 500 - 10,000. However, the data were so scattered that only a general trend of the interactions could be reflected (Rowe, 1961; Lee, 1979; Tsuji, 1982).

A micro-force measuring system was developed to directly measure the drag force on two interacting particles at a particle Reynolds number varying from 20 to 130. It was found that the particle Reynolds number affects not only the magnitude of the drag forces of an interacting particle but also its variation with the separation distance (Zhu, 1994). By using this experimental technique, the drag forces of interacting spheres in Newtonian fluid, have also measured by other authors (Liang, 1996; Chen, 2000).

The early study of particle dynamics in non-Newtonian flow can be dated back in early 1960s. However, the study of particulate non-Newtonian multiphase flow was not very active until 1990s. The drag coefficient of a single sphere in such kinds of pipe flow were determined by using the terminal velocity experiments of single sphere in various sized tubes filled with carboxymethycellulose (CMC) solution (Slattery, 1961).

An approximated momentum integral boundary layer analysis was concluded to determine the drag coefficient of a slow moving sphere in the creeping flow regime through a power-law non-Newtonian fluid in the presence of a flat wall (Acharya, 1976).

Most studies on the particle- particle interaction in non-Newtonian fluid have been theoretically restricted to the interaction during sedimentation (Lee, 2003).

In this study the hydrodynamic interaction is found experimentally in viscous and power - law fluid.

Hydrodynamic interaction of a pair of three-dimensional bodies moving in a uniform flow has been investigated by a number of researcher, the kinetic energy of the fluid, due to the motion of two spheres along the line joining their centers was analyzed and obtained solutions of added masses in terms of doublets interior to each body (Herman, 1987; Hick, 1880).

Considerable progress has been made towards the understanding of the accelerating motion of a sphere in Newtonian fluid; a concise summary of the theoretical developments on this subject have presented in the classic treatise of Clift *et al*. (1978). In contrast to this, the acceleration motion of a sphere in non Newtonian fluid has received less attention; some investigators have described the unsteady motion of a sphere in viscoelastic fluids.

The first attention to the acceleration motion of spherical particles in power law fluid was in 1991, in which a dense sphere is accelerated under gravity from rest in less dense liquid and ignored the effect of added mass and Basset force and through a numerical analysis to equation of motion charts were predicted to allow a priori estimation of the distance traveled to attain (99%) of its terminal velocity (Bagchi, 1991).

Through a numerical analysis to equation of motion of accelerated dense spheres in power law fluid from rest, the time and distance which required to reach (99%) of terminal velocity were predicted .The effect of added mass force was included but ignore the effect of Basset in the equation of motion of sphere and concluded that both dimensionless distance and time exhibited a stronger dependence on the flow behavior index for shear thinning fluid, they decrease with increasing power law index in the range of $10^{-2} \leq Re_{gn} \leq 10^{3}$, (Chhabra, 1998).

The drag force of two interacting spheres in power law fluid were measured by using a micro force measuring system and concluded that, while the drag force of an isolated sphere depends on the power law index, the drag coefficient ratio of an interacting sphere is independent of the power law index but strongly

depends on the separation distance and the particle Reynolds number $0.7 \leq \mathrm{Re}_{gn} \leq 23$, (Zhu, 2003).

For the time dependent motion, Oseen studied a falling spherical rigid inclusion in Newtonian fluid (Oseen, 1927).

The equation of motion of the sphere developed by Boussinesq, Basset and Oseen (BBO equation) may be written as follows:

$$F(t) = -6\pi\, a\mu_f (u) - \frac{1}{2} m_f \frac{d}{dt}(u) - 6a^2 \left(\pi\mu_f \rho_f\right)^{1/2} \int_0^t \frac{d}{d\tau} \frac{(u)}{(t-\tau)^{1/2}} d\tau \tag{1}$$

The oscillation of rigid sphere at Reynolds number up to 62 was studied experimentally to examine the acceleration effects on the motion of the particle, each contribution on the total unsteady drag of the sphere were measured separately and proposed modifying the BBO equation by multiplying respectively the three terms in right side of Eq. (1) by empirical coefficients, *CD*, *CVM* and *CH*. These coefficients depend on the particle Reynolds number (Re) and the acceleration number (Ac) (Odar, 1964).

$$Ac = \frac{u^2}{2a(du/dt)} \tag{2}$$

$$C_D = \frac{24}{\mathrm{Re}}\left(1 + 0.15\,\mathrm{Re}^{0.687}\right) \tag{3}$$

$$C_{VM} = 1.05 - \frac{0.066}{Ac^2 + 0.12} \tag{4}$$

And

$$C_H = 2.88 + \frac{3.12}{(Ac+1)^3} \tag{5}$$

So the modified of Eq. (1) is:

$$F(t) = -\frac{1}{2}\rho_f C_D \pi\, a^2 u^2 - C_{VM} m_f \frac{du}{dt} - C_H a^2 \left(\pi\, \mu_f \rho_f\right)^{1/2} \int_0^t \frac{du}{d\tau} \frac{d\tau}{(t-\tau)^{1/2}} \tag{6}$$

The use of these empirical coefficients has enabled accurate calculations of particle trajectories flow field at high Reynolds number (Odar, 1964).

For Newtonian fluid the drag coefficient is a unique function of Reynolds number, whereas in the case of power law fluid the drag coefficient may exhibit additional dependence on the power law flow behavior index.

In Newtonian fluid there are many correlations which are depending on the range of Reynolds number, for the considered range of spheres' Reynolds number (10 - $10^{3)}$, the widely used empirical form of drag correction with the Reynolds number employed is the Schiller and Naumann's correlation cited in Rowe and Henwood (1961).

$$C_D = \frac{24}{\mathrm{Re}}\left(1 + \frac{1}{6}\mathrm{Re}^{2/3}\right) \tag{7}$$

Kelessidis (2004) predicted the following drag coefficient correlation for power law fluid.

$$C_D = \frac{24}{\mathrm{Re}_{gn}}\left[1 + 0.1466\,\mathrm{Re}_{gn}^{0,378}\right] + \frac{0.44}{1 + 0.2635/\mathrm{Re}_{gn}} \quad 0.1 < \mathrm{Re}_{gn} < 10^3 \tag{8}$$

2. Experimental Apparatus and Measurement System:

The experimental apparatus is shown in Fig. (1). It consisted of a borosilicate glass cylindrical column of length 2.0 m and a diameter of 0.3 m. Two types of liquid were used in this study polyacrylamide (PAA) solution as a non Newtonian liquid type power law fluid with different concentrations (0.01,0.03, 0.05 and 0.07) % by weight and glycerin solution as Newtonian liquid with different concentration of (10, 20 , 30)% by weight. The spheres used in the experiments were made of stainless steel with different size (0.01, 0.012, 0.0134, and 0.016) m.

Each sphere pair was connected by using a thin steel rod with diameter approximately 1/50 of the sphere diameter. The effect of the existence of the connecting rod on the motion of the spheres may be considered to be negligible (Kumagai, 1989).

The distances between the spheres were varied from 2 to 10 radii. The spheres were suspended by a fishing string of 0.18 mm diameter, which passed over an aluminum pulley to a drive weight that provided the driving force.

External friction was reduced to a minimum with ball bearings on the pulley's shaft. The spheres were submerged in the solution of the column at an initial position of approximately 0.5 m from the bottom. Upon release of the string the spheres rose in the column under the action of falling weights. Measurements of the velocity of the pairs of spheres were carried out for different sphere diameters and sphere separation distances. On the top of the column there was a system of light source and a photo-cell. A small pieces of eight light blocks were fixed on the part of string which was un-submerged. As the spheres moved in the fluid, the light blocks also moved up through the collimator, which made the light intensity seen by the photo-cell varied and hence its resistance. This causes a variable voltage drop across the photo-cell. An electronic circuit was constructed to measure the time elapsed between two successive light blocks. The electronic circuit component consists of light source, photo-cell detector and the interface unit connected to the remote computer.

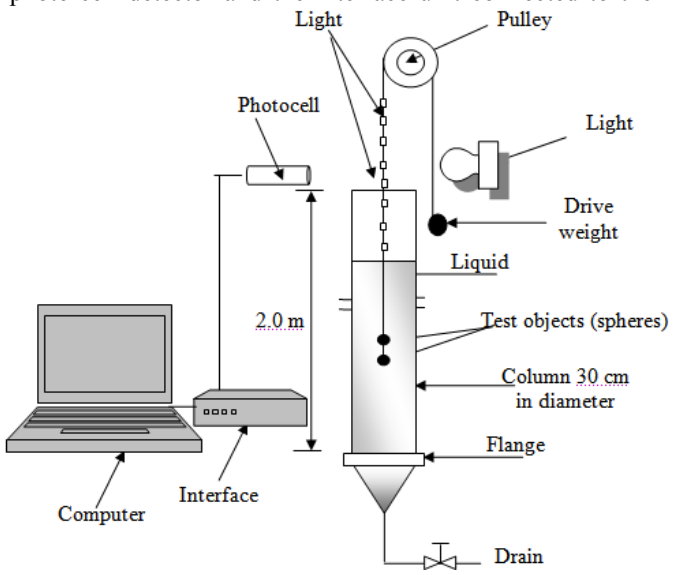

Fig. 1: Schematic diagram of experimental apparatus (Alwared, 2008; Mohammed, 2006).

3. Experimental Procedure:

For calibrating the system a single sphere submerged in the liquid column was accelerated under the action of a falling weight which was slightly heavier than the sphere. As the sphere moved up, the light blocks also moved up and passed between the light and the photo-cell. The interface unit fed the response to the computer until all light blocks were passed. The online computer printed the velocity of the spheres versus time on the screen.

Experimental procedure for two spheres is similar to the experiment with single sphere, the motion of two identical solid spheres rising along their line of centers and side by side was carried out for different sphere diameters and separation distances

Results and discussion

4.1drag Force:

In consistent with previous studies (Chhabra, 1998), it is assumed here that the drag coefficient of the accelerating sphere is similar to that under constant velocity. Eq. (7) was used to evaluate the drag coefficient in Newtonian fluid which is widely used empirical form of drag correction with the Reynolds number employed 10 - 10^3, and Eq. (8) was used to evaluate the drag coefficient for spheres in the power law fluid to take into account the effect of generated Reynolds number $1.1 \le \mathrm{Re}_{gn} \le 76$ and power law index 0.61 - 0.834 on the drag coefficient of the spheres.

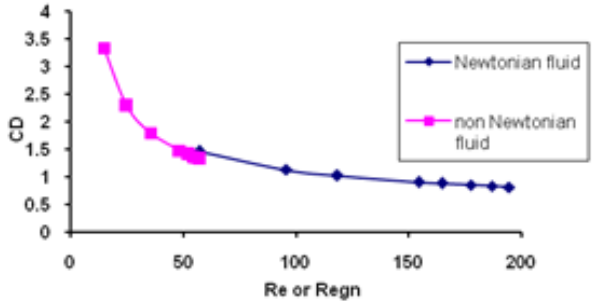

Fig. 2: Effect of Re and Re_{gn} on the drag coefficient for two steel spheres side by side in Newtonian and non Newtonian fluid.

The drag coefficient against Re and Re_{gn} for Newtonian and non Newtonian fluid for two side by side steel spheres (d=12mm, l/d=2) is plotted in Fig. (2).Comparing the C_D versus Re and Re_{gn} for Newtonian and non-Newtonian fluid on log-log scale, Fig. (3) reveals that good agreement between the Newtonian and non-Newtonian data for two spheres and that for a single sphere. It can be seen from this figure that drag coefficient decreases when the generated Reynolds number increases at the same liquid and as the shear thinning increases (power law index decreases).

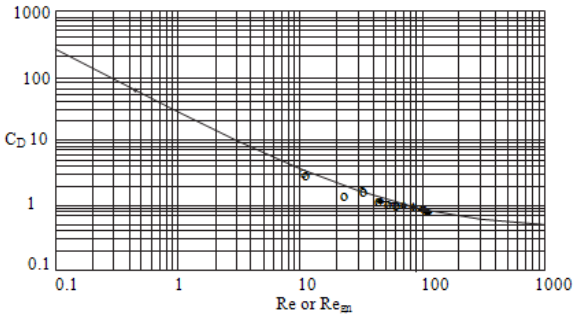

Fig. 3: Comparison of measurements of Newtonian and non-Newtonian data in log-log scale for two side by side steel spheres (d=12mm, l/a=2), in 0.01% PAA solution and 30% glycerin)
○ 0.01% PAA solution ◆ 30% glycerin solution — single sphere

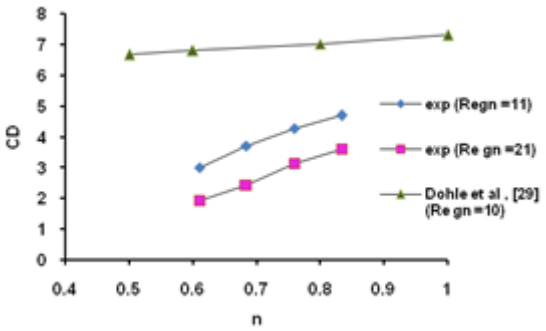

Fig. 4: Relationship between drag coefficient and power law index at constant generated Reynolds number for one steel sphere, d=10mm.

Fig. (4) shows the relationship between the drag coefficient and power law index at constant generated Reynolds number for one steel sphere (d=10mm) ,it can be seen from this figure that the drag coefficient increases with increasing power law index at constant generated Reynolds number and shows a fair agreement with the results of Dohle *et al.* (2006).

The dependency of the drag coefficient C_D on both generated Reynolds number and power-law index in the present study can be correlated as follows:

$$C_D = \frac{24}{\mathrm{Re}_{gn}}\left[1+0.16\,\mathrm{Re}_{gn}^{\frac{2.55n}{1.5n+2.35}}\right] \tag{9}$$

For Newtonian fluid n equals to unity, and Re = Re_{gn} therefore Eq. (9) becomes similar to Eq. (7).

4.2 Drag Force Correction Due to Interaction:

The interaction parameter ($\lambda = C_D / C_{DO}$) for both Newtonian and non-Newtonian fluid was calculated using Eq. (10) for two spheres moving side by side for $0.02 \le \mathrm{Re}_{gn} \le 500$[30].

$$\frac{C_D}{C_{Do}} = 1+\frac{1}{8}\left(\frac{l}{d}\right)^{-3} \tag{10}$$

The variation in the drag force of interacting spheres with the distance between the two spheres using Eq.(10) compared with Tsuji *et al*. (1982) experimental results are shown in Fig.(5).

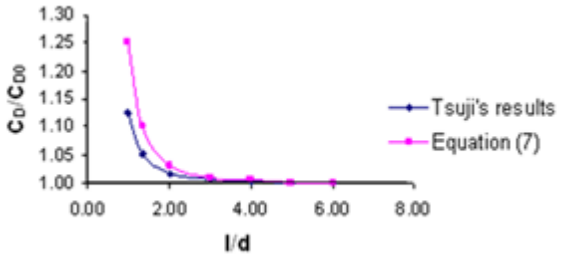

Fig. 5: Drag ratio versus inter-particle distance for two side by side spheres.

According to Kim *et al*. (1998) the drag increases as the two spheres get closer which is due to the increase of the shear stress on the sphere surface and the change in the pressure distribution owing to the flow acceleration in the gap between them.

The interaction parameter (λ) for two spheres moving in the direction parallel to their line of centers, the interaction parameter was calculated using Eq. (11) (Sulaymon, 2007).

$$\frac{C_D}{C_{Do}} = 1-\exp\left(-0.5\frac{l}{d}\right) \tag{11}$$

The data of Tsuji *et al.* (1982), Gluckman (1971) and Rowe and Henwood (1961) agrees very well with the predicted correlation as shown in Fig.(6).

To account for the effect of interaction on the drag force Eqs. (7) and (8) were multiplied by the drag correction (λ). The drag force (F_D) is then determined using:

$$F_D = \frac{1}{2}C_D\pi\rho_f a^2 u^2 \tag{12}$$

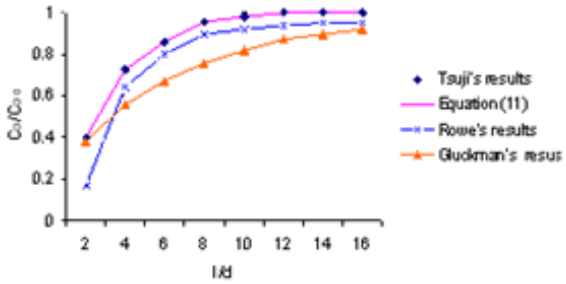

Fig. 6: Drag ratio as a function of inter-particle distance for two spheres moving along their line of centers.

Experimental studies suggest that the ratio of drag coefficients in power-law flow is exponentially dependent on the separation distance and is strongly related to the particle Reynolds number but nearly independent of the power-law index within the range of the present investigation. A similar behavior was observed by Zhu *et al*. (2003).

4.3 History Force Evaluation:

Expressions for the viscous drag force and the history force due to flow non-uniformity are of exactly the same form as the corresponding force constituents for that in an unbounded Newtonian fluid, save for the fluid viscosity and density being substituted by the effective viscosity and density (Siginer, 1999).

The literature revealed that the influence of the history force on the particle motion decreases with increasing particle density, and increasing particle size (Thomas, 1992) for that purpose the history force was evaluated for steel spheres of 16 mm in diameter in order to decrease the discrepancy.

The history force coefficient (C_H) is calculated by using equation (5) after obtaining the acceleration number (Ac) from equation (2) by using experimental values of the instantaneous velocity and acceleration.

$$\int_0^t \frac{du}{d\tau}\frac{d\tau}{(t-\tau)^{1/2}} = \sum_{n=0}^{m-1}\frac{u^{n+1}-u^n}{\Delta t_n} 2\left(\sqrt{t-t_n}-\sqrt{t-t_{n+1}}\right) \tag{13}$$

Where the counter 0,...,m refers to the successive solutions points in the interval [0,t] and n is the number of time intervals. This equation was developed by Alexander (2004) for each time interval the value of $\frac{du}{dt}$ is multiplied by the corresponding $2\left(\sqrt{t-t_n}\right)$. The history force is then calculated from:

$$F_H = C_H\left(\pi\mu_{APP}\rho_f\right)^{1/2} a^2 \int_0^t \frac{du}{d\tau}\frac{d\tau}{(t-\tau)^{1/2}} \tag{14}$$

In order to quantify the effect of fluid rheology on the history force, it is important to evaluate the effect of power law index on the history force; Fig. (7) illustrates the variation of history force with time at different power law index.

It can be seen also from this figure that the values of history force for different power law index are very close and there is no clear effect of power law index on the history force so the history force is not significantly altered by fluid rheology. This behavior was found to be the same for the different configuration.

Fig. (8) shows the change of the history force with time for Newtonian and non Newtonian fluid. The history force decays faster then t^{-2}, the same behavior was observed by Lawrence and Mei (1995) and Mordant and Pinton (2000).

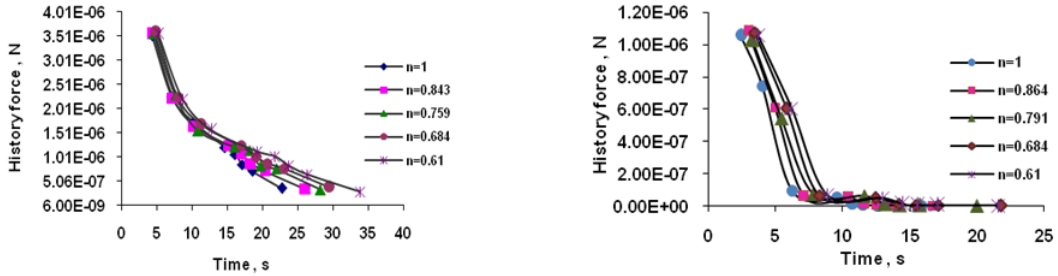

(a)Two spheres side by side (b) Two spheres in line

Fig. 7: Effect of power law index on the history force.

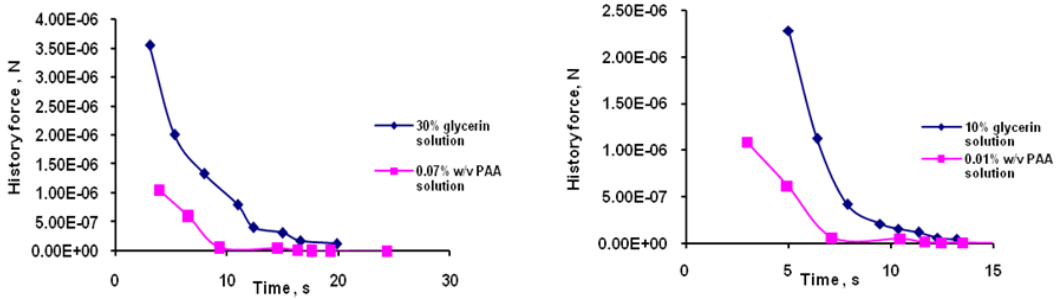

(a)Two spheres side by side (b) Two spheres in line

Fig. 8: The change of history with time for side by side spheres (d=12 mm, l/a =2).

4.4 Virtual Mass Evaluation:

For two equal spheres moving side by side, Fig. (9) Shows that when the spheres touch (*l/a* =2), the virtual mass coefficient (C_{VM}) is greater than 0.5 for both Newtonian and non Newtonian fluid. As the distance between the spheres increases, the virtual mass coefficient decreases asymptotically and approaches the single sphere value (i.e. C_{VM}= 0.5). This value is attained when the spheres are separated by more than 6 radii for Newtonian fluid and more than 10 radii for non Newtonian fluid.

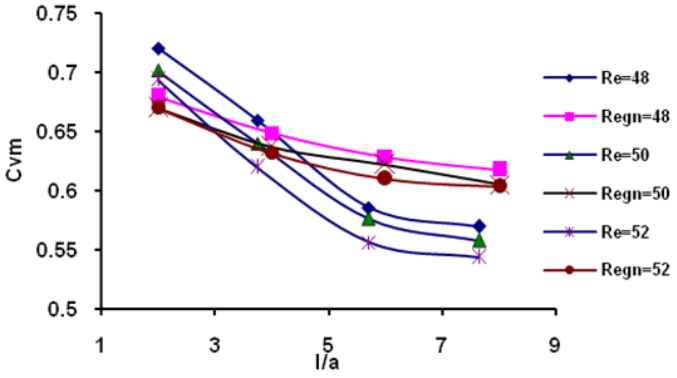

Fig. 9: Virtual mass coefficient versus inter- particle distance for two side by side spheres in 30% glycerin and 0.01% PAA solutions.

For two equal spheres moving along the line joining their centers Fig. (10) shows that when the spheres touch, the virtual mass coefficient is less than 0.5, it increases rapidly as the distance between the spheres increases. At larger separation it asymptotically approaches the single sphere value of 0.5 at separation distances more than 5 radii for Newtonian fluid and more than 10 radii for non Newtonian fluid.

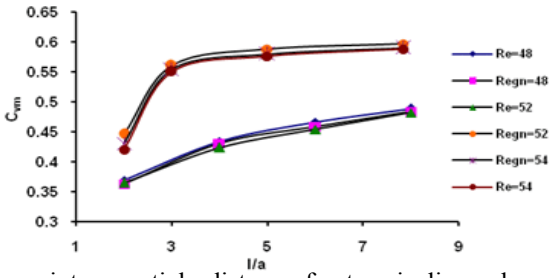

Fig. 10: Virtual mass coefficient versus inter- particle distance for two in line spheres in 30% glycerin and 0.01% PAA solutions.

It can be concluded that due to the rheological properties of the non Newtonian fluid, it requires the two spheres to be separated farther than in Newtonian fluid in order to approach the single sphere behavior.

For two spheres moving side by side, the present experimental C_{VM} can be correlated to the inter-particle distance and Reynolds number as follows:

$$C_{VM} = \frac{1}{2}\left[1+\frac{3}{2}\left(\frac{l}{a}\right)^{-3}\right] + A\,\mathrm{Re}^{-B} \tag{15}$$

For two spheres moving along the line joining their centers, the experimental values of C_{VM} can be correlated to the inter-particle distance and Reynolds number as follows:

$$C_{VM} = \frac{1}{2}\left[1-3\left(\frac{l}{a}\right)^{-3}\right] + A\,\mathrm{Re}^{-B} \tag{16}$$

where :
A = 0.477, B = 0.754 at Re = Re_{gn} for PAA solution, and A = 15, B = 1.125 for glycerin solution. The first term of the above equations shows the dependency of C_{VM} on the inter-particle distance. The second term represents the effect of Reynolds number; it was found that the value of C_{VM} varies inversely with Reynolds number.

Conclusions:

The drag coefficient of two spheres at different configurations decreases when Reynolds number or generated Reynolds number increases for both Newtonian and non Newtonian fluid.

The drag coefficient ratio of interacting spheres is independent of the power law index but strongly depends on the separation distance and the particle Reynolds number. Newtonian fluid correlations were used to predict an expression that relates the drag coefficient with the inter-particle distance in power law fluid.

The drag coefficient increases with increasing power law index at constant generated Reynolds number. The dependency of the drag coefficient C_D on both generated Reynolds number and power-law index in the present study can be correlated as follows:

$$C_D = \frac{24}{\mathrm{Re}_{gn}}\left[1+0.16\,\mathrm{Re}_{gn}^{\frac{2.55n}{1.5n+2.35}}\right] \tag{9}$$

The change of the history force with time for Newtonian and non Newtonian fluid shows decays faster then t^{-2}.

Due to the rheological properties of the non Newtonian fluid it requires the two spheres to be separated farther than in Newtonian fluid in order to approach the virtual mass coefficient of single sphere.

Nomenclature:

a	Sphere radius, m	x	Distance between sphere surfaces, m
A_C	Acceleration number,-	Re_{gn}	Generated Reynolds number for power law fluid, $\rho V^{2-n} d^n / k$
C_D	Drag coefficient,-		
C_{Do}	Drag coefficient of an isolated sphere,-	S	Dimensionless separation)l/a(
C_H	History coefficient,-	t	Time, s
C_M	Inertial coefficient (1+ C_{VM}) ,-	u	Sphere velocity, m/s
C_{VM}	Virtual mass coefficient,-	V	Fluid velocity, m/ s
D	Sphere diameter, m	Vs	Volume of sphere, m^3
F_B	Buoyancy force, N		
F_D	Drag force, N	*Greek letters*	
F_H	History force, N	μ	Viscosity, kg/m. s
F(t)	Hydrodynamic force, N	μ_{app}	Apparent viscosity, kg/m. s
F_{VM}	Virtual mass force, N	τ	Dummy time variable, s
g	Gravitational acceleration, m/s^2	Δt	Time step, s
l	Distance between the centers of spheres, m	λ	Drag interaction parameter (C_D /C_{Do})-
M_{drive}	Drive weight, kg	μ_f	Dynamic viscosity of fluid, kg/m. s
n	Power law index (flow behavior index)-	ρ_s	Density of sphere, kg/m^3
k	Consistency index, (Pa. s^n)	ν_f	Kinematic viscosity of fluid (μ_f /ρ_f), m^2/ s
Re	Reynolds number based on the sphere diameter (u d/ ν_f)	ρ_f	Density of fluid, kg/m^3

References

Acharya, A., R.A. Mashelkar, J. Ulbrecht, 1976. Flow of inelastic and viscoelastic fluids past a sphere –I. Drag coefficient in creeping and boundary-layer flows. Rheol. Acta, 15: 454.

Alwared, A.I., 2008. Hydrodynamic of Spheres in Various Solutions, PhD Thesis, Baghdad University.

Alexander, P., 2004."High Order Computation of the History Term in the Equation of Motion for a Spherical Particle in a Fluid, J. of Scientific Computing, 21(2): 129-143.

Bagchi, A. and R.P. Chhabra, 1991. Acceleration motion of spherical particles in power law type non Newtonian liquids", J. of powder technology, 68: 85-90.

Chen, R.C., J.L. Wu, 2000. The flow characteristics between two interactive spheres. Chem. Eng. Sci., 55: 1143.

Clift, R., J.R. Grace and M.E. Weber, 1978 Bubbles, Drops and Particles, Academic Press, New York.

Chhabra, R.P., A. Soares and J.M. Ferreira, 1998. A Numerical Study of the Accelerating Motion of a Dense Rigid Sphere in non Newtonian Power Law Fluids , The Canadian Journal of chemical Engineering , 76: 1051-1055.

Dhole, S.D., R.P. Chhabra And V. Eswaran, 2006. Flow of Power-Law Fluids Past a Sphere at Intermediate Reynolds Numbers , Ind. Eng. Chem. Res., 45(13): 4773 -4781.

Greenstein, T., 1980. Interaction and wall corrections for the slow motion of two fluid or solid particles parallel to the axis of a circular cylinder through a viscous fluid. J. Mech. Eng. Sci., 22: 243.

Gluckman, J., R. Pfeffer and S. Weinbaum, 1971. A New Technique for Treating Multi-particle Slow Viscous Flow: Axisymmetric Flow past Spheres and Spheroids, J. Fluid Mech., 50: 705-740.

Happel, J. and R. Pfeffer, 1960. The Motion of Two Spheres Following each other in a Viscous Fluid, AIChE J., 6(1): 129-133.

Herman, R.A., 1887. On the motion of two spheres in fluid, Quart. J. Pure Appl. Math., 22: 204-216.

Hick, W.M., 1880. On the motion of two spheres in a fluid, Phil. Trans. Roy. Soc., 171: 455-492.

Kaneda, Y., K. Ishii, 1982. The hydrodynamic interaction of two spheres moving in an unbounded fluid at small but finite Reynolds number, J. Fluid Mech., 124: 209.

Kynch, G.J., 1959. The Slow Motion of Two or More Spheres through a Viscous Fluid, J. of Fluid Mech., 5: 193-208.

Kelessidie, V., 2004. Measurements and Prediction of Terminal Velocity of Solid Spheres Falling through Stagnant Pseudoplastic Liquids, J. of Powder Technology, 147: 117-125.

Kumagai, T. and M. Muraoka, 1989. On the motion of spheres in a fluid at low Reynolds number, JSME Int. J., 32: 309-316.

Kim, I., S. Elghobashi and W.A. Sirignano, 1998. On the Equation for Spherical Particle Motion: Effect of Reynolds and Acceleration Numbers, J. Fluid Mech., 367: 221-253.

Lee, K.C., 1979. Aerodynamic Interaction between Two Spheres at Reynolds Numbers around 10^4, Aeronaut Q., 30: 371-385.

Liang, S.C., T. Hong and L.S. Fan, 1996. Effects of Particle Arrangements on the Drag Force of a Particle in the Intermediate Flow Regime, Int. J. of Multiphase Flow, 22(2): 285-306.

Lee, S.W., S.H. Ryu and C. Kim, 2003. Studies on the Axisymmetric Sphere-Sphere interaction problem in Newtonian and non-Newtonian fluids, J. of non Newtonian Fluid Mechanic, 110: 1-25.

Legendre, D., J. Magnaudet and G. Mougin, 2003. Hydrodynamic Interactions between Two Spherical Bubbles Rising Side by Side in a Viscous Liquid, J. of Fluid Mech., 497: 133-166.

Lawrence, C.J. and R.W. Mei, 1995. Long-time Behavior of the Drag on a Body in an Impulsive Motion, J. of Fluid Mech., 283: 307-327.

Mordant, N. J.F. Pinton, 2000. Velocity Measurement of a Settling Sphere, Eur. J. Phys. B., 18: 343-352.

Mohammed, S.A.M., 2006. Hydrodynamic Interaction between Two Spheres, Ph.D. thesis, Dept. of Chem. Eng., College of Engineering, University of Baghdad.

Oseen, C., 1927.Hydrodynamik, Akademische, Leipzig.

Odar, F. and W.S. Hamilton, 1964. Forces on a Sphere Accelerating in a Viscous Fluid, J. Fluid Mech., 18: 302-314.

Payne, L.E. W.H. Pell, 1960. The Stokes Flow Problem for a Glass of Axially Symmetric Bodies, J. Fluid Mech., 7: 529.

Rowe, P.N. and G.A. Henwood, 1961. Drag Forces in a Hydraulic Model of a Fluidized Bed-Part I, Trans. Instn. Chem. Engrs., 39: 43-54.

Stimson, M. and G.B. Jeffery, 1926. The Motion of Two Spheres in a Viscous Fluid, Proc. Roy. Soc., A111: 110-116.

Slattery, J.C., R.B. Bird, 1961. Non-Newtonian flow past a sphere. Chem. Eng. Sci., 16: 231.

Sulaymon, A.H. and S.M.M. Mohammed, 2007. Drag Forces under Longitudinal Interaction of Two Spheres, Iraqi J. Chem. And Petro. Eng., 8(2): 1-4.

Siginer, D.A., D. Kee and R.P. Chhabra, 1999. Advances in the F low and Rheology of Non- Newtonian Fluids, Elsever.

Tsuji, Y., Y. Morikawa and K. Terashima, 1982. Fluid-dynamic Interaction between Two Spheres, Int. J. Multiphase Flow, 8: 71-82.

Thomas, P.J., 1992. On the Influence of the Bassety History Force on the Motion of a Particle through a Fluid, Phts. Fluids A 4(9): 2090-2093.

Zhu, C., K. Lam, X. Tang and G. Liu, 2003. Drag forces of interacting spheres in power-law fluids, Journal of mechanics research communications, 30: 651-662.

Zick, A.A., G.M. Homsy, 1982. Stokes Flow Through Periodic Arrays of Spheres, J. Fluid Mech., 13: 115.

Zhu, C., S.C. Liang and L.S.Fan, 1994. Particle Wake Effect on the Drag Force of an Interactive Particle, Int. J. Multiphase Flow, 20: 117-129.